

Low-Dose CT in Lung Pathologies Related to Rheumatoid Arthritis: Comparison of Deep Learning-Based Noise Reduction Algorithm and Iterative Reconstruction Algorithm

Original Article

Aybuke Uçar¹, İnan Korkmaz²

1. Suruç State Hospital, Department of Radiology
2. Hatay Mustafa Kemal University, Faculty of Medicine, Department of Radiology

ABSTRACT

Aim: Conventional CT scans may require high radiation doses, which can cause undesirable effects, therefore, the use of low-dose CT scans has become increasingly important. The aim of this study is to compare the effectiveness of a deep learning-based noise reduction algorithm and an iterative reconstruction algorithm in the evaluation of lung pathologies observed in patients diagnosed with RA using low-dose CT.

Methodology: Standard dose CT scans and low dose CT scans (Precise 30 mAs and 45 mAs) obtained with deep learning-based noise reduction method of patients followed up with the diagnosis of rheumatoid arthritis were evaluated in terms of visual quality, image noise and contrast-to-noise ratio.

Results: In the visual assessment scoring, standard dose imaging and Precise 45 mAs images were found to be statistically compatible, but there was a discrepancy in the 30 mAs images. Image noise was found to be statistically significantly higher in both the mediastinum and parenchymal windows in 30 mAs images ($p<0.001$). Post-hoc evaluations of CNR revealed that the CNR values of standard and Precise 45 mAs imaging in the mediastinal window were similar, while Precise 30 mAs imaging had a statistically significantly lower CNR value ($p<0.001$). Significant differences were found in total DLP values among all three imaging protocols ($p<0.001$).

Conclusion: In evaluating the image quality obtained with different dose protocols in low-dose thoracic CT scans of patients diagnosed with RA, it was observed that the deep learning-based reconstruction algorithm provided diagnostically reliable results, especially at the 45 mAs level.

Keywords: Low-dose chest CT; Image quality evaluation; Deep learning-based noise reduction; Radiation dose

Introduction

Rheumatoid arthritis (RA) is a systemic disease characterized by chronic inflammation, particularly in the small

joints. In the long term, RA affects not only joint structures but also various internal organs. The lungs are among these organs, and pulmonary manifestations of RA include interstitial lung disease, nodules,

and pleural effusion. Such complications not only significantly reduce the quality of life of patients but also may increase morbidity and mortality rates (1).

Imaging techniques play a critical role in the evaluation of lung pathologies in patients diagnosed with RA. In this context, computed tomography (CT) is an important tool with the potential to examine changes in the lungs in detail. However, conventional CT scans may require high radiation doses, which can cause undesirable effects, especially in RA patients requiring long-term follow-up. Therefore, the use of low-dose CT scans has become increasingly important (2).

In recent years, artificial intelligence and deep learning techniques in medical imaging have attracted attention for their potential to improve image quality while minimizing radiation dose. Deep learning-based noise reduction algorithms, in particular, can significantly improve the quality of data obtained from low-dose CT images. These algorithms reduce unwanted noise in images and enable clearer and more detailed results (3).

Iterative reconstruction algorithms are another innovative method used in low-dose CT scans. These algorithms utilize data more effectively during the image formation process and can produce higher-quality images at lower doses compared to conventional reconstruction techniques. Comparing the effectiveness and reliability of both types of algorithms can reveal their potential in the management of patients with RA (4).

The aim of this study is to compare the effectiveness of a deep learning-based noise reduction algorithm and an iterative reconstruction algorithm in the evaluation

of lung pathologies observed in patients diagnosed with RA using low-dose CT. This study seeks to determine the appropriate method and radiation dose level for achieving diagnostic imaging with reduced radiation exposure by comparing the effects of both algorithms on image quality.

Materials and Methods

This retrospective study was approved by Ethics Committee of Mustafa Kemal University, and the requirement for informed consent was waived (30/04/2025, meeting no. 6, decision no. 39). The study protocol complies with the ethical guidelines of the 1975 Declaration of Helsinki, which the institution's human research committee previously approved.

2.1. Patient Selection

The sample of the study included a total of 26 patients, 19 women and 7 men, who were diagnosed with RA in the Rheumatology Department and underwent CT imaging for the monitoring of lung pathologies. The ages of the patients ranged from 40 to 76 years. Their mean BMI value was 27.4 ± 4.5 . Patients younger than 18 years, those with a history of lung surgery, those with pulmonary diseases other than RA, and those without optimal-quality CT images were excluded.

2.2. CT Imaging

Standard scans were performed using the iterative reconstruction technique (IRT), while new low-dose scans were obtained using the deep learning-based noise reduction method (Precise) at 30 and 45 mAs doses. All images were obtained with a 128-slice Philips Incisive CT scanner. Scans were performed in the caudocranial direction, in the supine position, and

without contrast material. Reconstructions with deep learning-based noise reduction were performed at fixed 30 mAs and 45 mAs doses using the Philips Precise Image program. The scan parameters were as follows: collimation value: 64×0.625 , pitch value: 1.00, and gantry rotation time: 0.50 seconds. Slice thickness was standardized at 1 mm.

2.3. Image Analysis

The standard scans obtained with the iterative reconstruction algorithm (IRT) were available in the hospital's PACS system, and the comparative evaluation of the images of the patients obtained with the deep learning-based noise reduction method (Precise), also available in the system, was performed.

The total DLP doses of the standard, Precise 30 mAs, and Precise 45 mAs scans of the patients were recorded. The images of all patients were evaluated for rheumatoid nodules, bronchiectasis, reticulation, and

honeycombing. In both standard and low-dose (Precise) examinations, the image quality regarding existing lung pathologies was compared.

2.4. Objective Image Measurements

Image noise was measured by placing a standard-sized ROI in the tracheal lumen just superior to the tracheal carina in the parenchymal window (WL: -600, WW: 1600) and in the aortic lumen at the level of the aortic arch in the mediastinal window (WL: 300, WW: 1500) (Figure 1). Noise was defined as the standard deviation (SD) of attenuation within the ROI. The contrast-to-noise ratio was calculated using the formula $CNR-M = HU_{adipose\ tissue} - HU_{aorta} / SDA_{aorta}$ in the mediastinal window, based on the mean HU values of adipose tissue and the aorta, and $CNR-P = HU_{parenchyma} - HU_{trachea} / SD_{trachea}$ in the parenchymal window, based on the mean HU values of parenchyma and trachea.

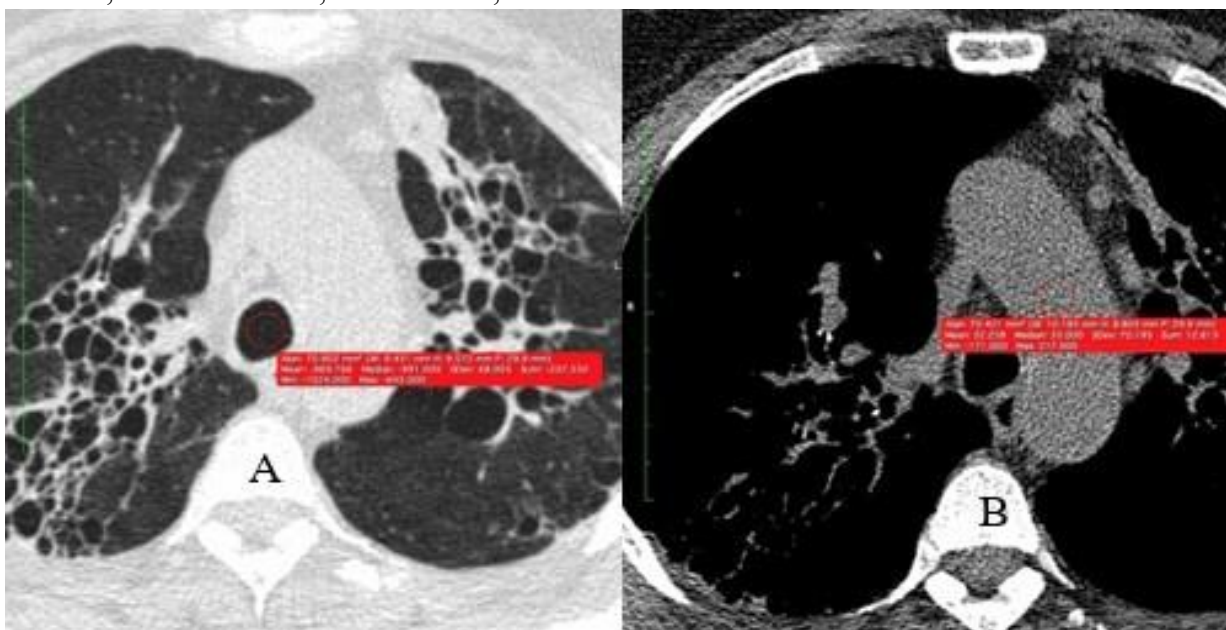


Figure 1. Image noise measurements were performed with standard-sized ROIs from the tracheal lumen (A) just superior to the carinal level in the parenchymal window, and from the aortic arch level (B) in the mediastinal window.

Visual quality parameters were established by reviewing studies in the literature conducted for different pathologies in the field of thoracic radiology. Visual quality assessments were performed by two radiologists (14 years and 5 years of experience), and consensus was reached for visual scores. The evaluation was based on five parameters: lesion edge sharpness (LES), visibility of small structures (VSS), visual noise (VN), artifacts (ART), and diagnostic reliability (DR). Scoring was applied as follows: 1 = Non-diagnostic, 2 = Low quality, 3 = Moderate quality, 4 = Good quality, and 5 = Excellent quality.

2.6. Statistical Analysis

All statistical analyses were performed using IBM SPSS Statistics version 27.0 (IBM Corp., Armonk, NY, USA). The normality of the distribution of the continuous variables was assessed with the Shapiro-Wilk test. Variables with normal distribution are presented with mean \pm standard deviation values, while those without normal distribution are presented with median (minimum-maximum) values. Since visual assessment scores were ordinal in structure, and three protocols (standard, 30 mAs, and 45 mAs) were compared, the Friedman test for dependent groups was used. For parameters found significant in the Friedman test, post hoc pairwise comparisons were performed using the Least Significant Difference (LSD) test. Different superscripts (A, B, C) indicate statistically significant differences between groups ($p < 0.05$). The visual quality scores of patients with body mass index (BMI) < 30 and ≥ 30 for the 30 mAs and 45 mAs protocols were compared separately for

each parameter. In these comparisons, since visual scores were categorical and ordinal, and the number of observations in some cells was low, p-values were obtained using the chi-squared test, or where appropriate, the Fisher-Freeman-Halton test. A significance level of $p < 0.05$ was accepted for all statistical analyses.

Results

This was a retrospective study. A total of 26 patients, 19 women and 7 men, were included. The ages of the included patients ranged from 40 to 76 years. The mean BMI value of the patients was 27.4 ± 4.5 kg/m².

In the objective evaluations, the mean image noise values measured from the tracheal lumen (MN-T) in the parenchymal window and the aortic arch (MN-A) in the mediastinal window were calculated separately for each imaging protocol. In the Precise 30 mAs protocol, both MN-T and MN-A values were observed to be markedly high. The lowest image noise values were detected in standard (IRT) scans, while the Precise 45 mAs protocol provided intermediate values in this respect. As expected, total DLP values increased in the following order: Precise 30 mAs $<$ Precise 45 mAs $<$ IRT scans. The mean noise values, CNR, and total DLP results are summarized in Table 1.

In visual scoring, each parameter specified in the subjective image analyses was evaluated separately for Precise 30 mAs, Precise 45 mAs, and IRT (standard dose) HRCT scans (Table 2).

In the statistical analyses, no statistically significant difference was found between the standard scans and the Precise 45 mAs

protocol in terms of visual assessment scores, as indicated by the superscripts. These two protocols were found to be consistent with each other in the visual evaluations. Nevertheless, there was a

statistically significant difference ($p < 0.001$) and inconsistency between Precise 30 mAs scans and both Precise 45 mAs scans and standard HRCT scans (Figure 2).

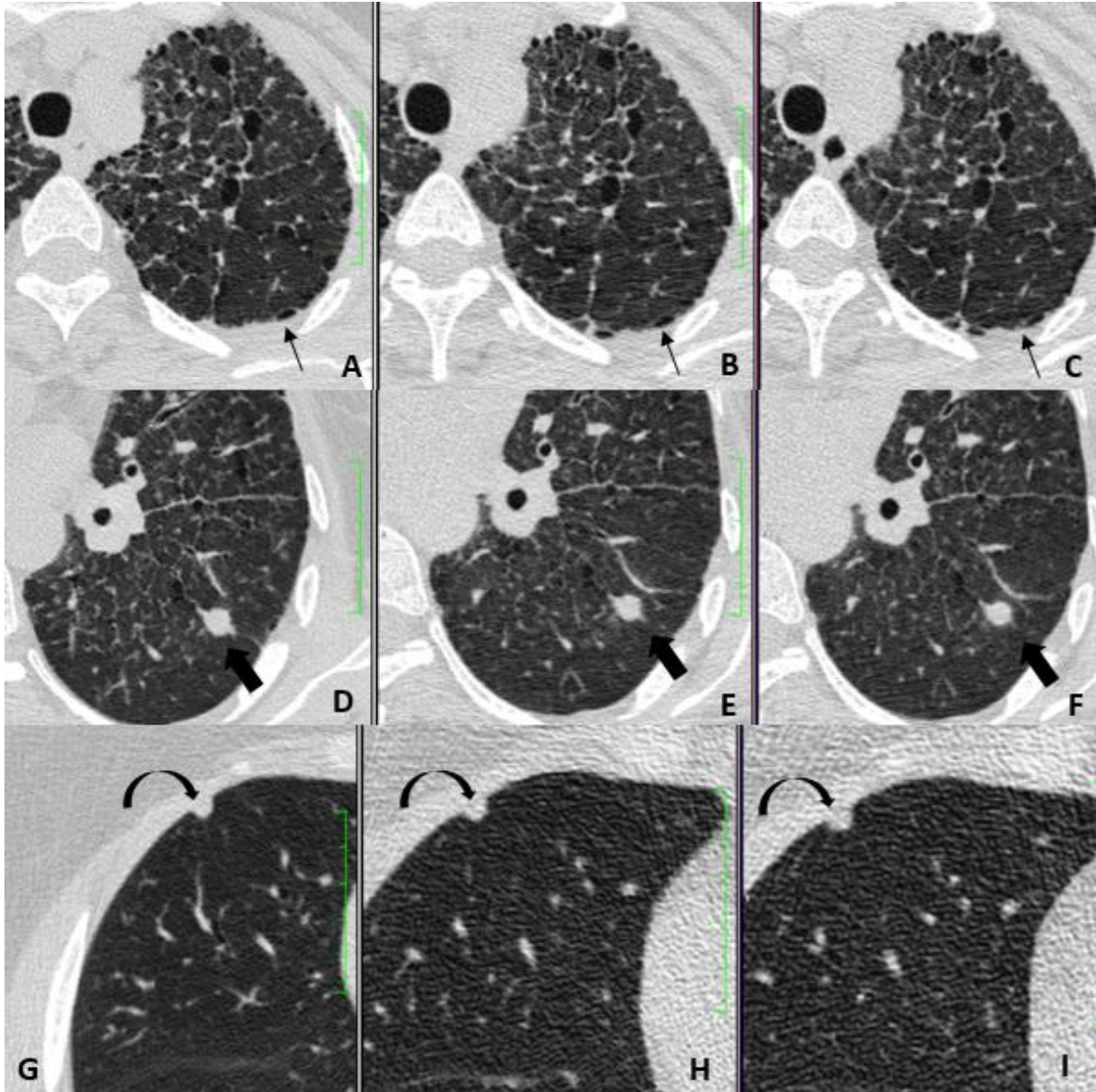


Figure 2. In a patient with reticulation, septal thickening, and air cysts (A, B, C); there is no marked difference in visual evaluations between the standard (A) and 45 mAs (B) images, while in the 30 mAs (C) images, a slight loss of sharpness is observed in small subpleural pathologies (black arrow). In a patient with a nodule (D, E, F); in the 45 mAs (E) image, compared to the standard image (D), a relative decrease is observed in the edge sharpness of the nodule and small structures, while in the 30 mAs (F) image, blurring of the nodule edges and haziness around it are present (thick arrow). In another patient with a nodule (G, H, I); compared to the standard image (G), in the 45 mAs (H) and more prominently in the 30 mAs (I) images, there is an increase in image noise, a decrease in nodule edge sharpness (curved arrow), and reduced visibility of small structures.

In the quantitative evaluations, significant differences were found among all three imaging protocols in terms of image noise measured from the tracheal level (MN-T) in the parenchymal window and the aortic level (MN-A) in the mediastinal window, as well as total DLP values ($p < 0.001$). In particular, in the 30 mAs protocol, image noise increased markedly at both tracheal and aortic levels, and this difference was statistically significant. However, despite this increase, it was observed that diagnostic quality could be tolerated in visual scoring. All these results are summarized in Table 3.

In mediastinal and parenchymal window CNR evaluations, the CNR values of the standard, Precise 30 mAs, and Precise 45 mAs scans were found to differ

significantly ($p < 0.001$). The post hoc analyses revealed that in the mediastinal window, the CNR values of standard and Precise 45 mAs imaging were similar, while Precise 30 mAs imaging showed significantly lower CNR values. In the parenchymal window, post hoc analyses showed that Precise 30 mAs images had significantly lower values than Precise 45 mAs images, and Precise 45 mAs images had significantly lower values than standard scans (Table 4).

In the statistical analyses of the visual scores of patients divided into two groups according to BMI (< 30 and ≥ 30 kg/m²) for the Precise 30 mAs and Precise 45 mAs scans, no statistically significant difference was found between the groups in either imaging protocol.

Table 1. Mean Noise Values, CNR, and Total DLP Results in Standard and Low-Dose Scans

	X	SD
MN-T (Standard) [HU]	46.0	13.1
MN-A (Standard) [HU]	67.5	27.4
CNR-P (Standard)	2.59	
CNR-M (Standard)	2.34	
DLP (Standard) [mGy·cm]	591.8	199.7
MN-T (Precise 45 mAs) [HU]	63.2	24.4
MN-A (Precise 45 mAs) [HU]	105.0	49.3
CNR-P (Precise 45 mAs)	1.96	
CNR-M (Precise 45 mAs)	1.67	
DLP (Precise 45 mAs) [mGy·cm]	94.1	11.0
MN-T (Precise 30 mAs) [HU]	76.5	31.4
MN-A (Precise 30 mAs) [HU]	128.3	55.2
CNR-P (Precise 30 mAs)	1.66	
CNR-M (Precise 30 mAs)	1.20	
DLP (Precise 30 mAs) [mGy·cm]	62.4	6.6

Table 2. Distribution of Scores for Visual Quality Assessment Parameters (LES, VSS, VN, ART, and DR) by Observer in Standard and Precise Scans

	NON-DIAGNOSTIC	LOW QUALITY	MODERATE QUALITY	GOOD QUALITY	EXCELLENT QUALITY
STANDARD					
LES	0 (0.0%)	1 (3.8%)	4 (15.4%)	10 (38.5%)	11 (42.3%)
VSS	0 (0.0%)	1 (3.8%)	3 (11.5%)	5 (19.2%)	17 (65.4%)
VN	0 (0.0%)	0 (0.0%)	5 (19.2%)	14 (53.8%)	7 (26.9%)
ART	0 (0.0%)	2 (7.7%)	5 (19.2%)	16 (61.5%)	3 (11.5%)
DR	0 (0.0%)	0 (0.0%)	3 (11.5%)	8 (30.8%)	15 (57.7%)
Precise 30 mAs					
LES	1 (3.8%)	5 (19.2%)	12 (46.2%)	7 (26.9%)	1 (3.8%)
VSS	1 (3.8%)	4 (15.4%)	8 (30.8%)	10 (38.5%)	3 (11.5%)
VN	0 (0.0%)	7 (26.9%)	14 (53.8%)	5 (19.2%)	0 (0.0%)
ART	0 (0.0%)	4 (15.4%)	6 (23.1%)	15 (57.7%)	1 (3.8%)
DR	1 (3.8%)	2 (7.7%)	7 (26.9%)	12 (46.2%)	4 (15.4%)
Precise 45 mAs					
LES	0 (0.0%)	1 (3.8%)	5 (19.2%)	10 (38.5%)	10 (38.5%)
VSS	0 (0.0%)	1 (3.8%)	4 (15.4%)	7 (26.9%)	14 (53.8%)
VN	0 (0.0%)	0 (0.0%)	7 (26.9%)	16 (61.5%)	3 (11.5%)
ART	0 (0.0%)	0 (0.0%)	5 (19.2%)	17 (65.4%)	4 (15.4%)
DR	0 (0.0%)	0 (0.0%)	3 (11.5%)	3 (11.5%)	20 (76.9%)

Table 3. Comparison of Visual Scores and Quantitative Noise Values

	Standard M [Q1-Q3]	Precise 30 mAs M [Q1-Q3]	Precise 45 mAs M [Q1-Q3]	p-value
LES	^A 4 [4 - 5]	^B 3 [3 - 4]	^A 4 [4 - 5]	<0.001
VSS	^A 5 [4 - 5]	^B 3,5 [3 - 4]	^A 5 [4 - 5]	<0.001
VN	^A 4 [4 - 5]	^B 3 [2 - 3]	^A 4 [3 - 4]	<0.001
ART	^A 4 [3 - 4]	^B 4 [3 - 4]	^A 4 [4 - 4]	0.001
DR	^A 5 [4 - 5]	^B 4 [3 - 4]	^A 5 [5 - 5]	<0.001
MN-T [HU]	^A 43.87 [35.68 - 53.43]	^C 74.64 [50.96 - 94.62]	^B 57.33 [46.3 - 78.6]	<0.001
MN-A [HU]	^A 64.84 [55 - 75.15]	^C 122.99 [89.62 - 175.77]	^B 96.02 [69 - 140.8]	<0.001
Total DLP	^C 532.63 [492.13 - 624.2]	^A 62.51 [56.86 - 67.57]	^B 93.8 [85.57 - 101.77]	<0.001

p-Values are obtained from the Friedman test. Post hoc pairwise comparisons are made using the LSD test. Different letters in superscripts (A,B,C) indicate statistical significance ($p < 0.05$).

Table 4. Analysis of CNR Values

	Standard M [Q1-Q3]	Precise 30 mAs M [Q1-Q3]	Precise 45 mAs M [Q1-Q3]	p
CNR-M	^B -2.34 [-2.75 - -1.89]	^A -1.20 [-1.80 - -0.81]	^B -1.67 [-2.25 - -1.02]	<0.001
CNR-P	^C 2.59 [1.97-3.03]	^A 1.66 [0.87-2.09]	^B 1.96 [1.30-2.54]	<0.001

p-Values are obtained from the Friedman test. Post hoc pairwise comparisons are made using the LSD test. Different letters in superscripts (A,B,C) indicate statistical significance ($p < 0.05$).

Discussions

In this study, the effects of low-dose CT scans obtained with a deep learning-based noise reduction algorithm and those obtained with an iterative reconstruction algorithm on image quality in the thoracic imaging of patients diagnosed with RA were compared.

In light of our review of the literature, this study is a pioneering study evaluating the

diagnostic adequacy of low-dose CT protocols in patients with RA, which aimed to provide a foundation for further research in this field.

In 2024, Hackner et al. published a Delphi-based consensus study emphasizing the importance of high-resolution CT (HRCT) as the primary screening method in the diagnosis of RA-associated interstitial lung disease (RA-ILD). They reported that HRCT could be considered for early

screening even in asymptomatic patients according to risk factors, but its routine use should be carefully evaluated on a patient-by-patient basis due to radiation exposure concerns (5).

Although low-dose CT imaging provides an advantage in reducing radiation dose, radiation exposure remains a concern in young and pediatric patients, as well as in patients with RA who undergo repeated CT examinations.

Brenner and Hall (2007) emphasized that the rapidly increasing use of CT in recent years has significantly raised the amount of ionizing radiation to which the population is exposed, noting that radiation doses per organ in abdominal CT scans are tens of times higher compared to those seen in conventional radiological methods (6). In this context, evaluating the diagnostic adequacy of images obtained with low-dose CT scans (30 mAs and 45 mAs protocols) in our study is important both for patient safety in clinical practice and for public health.

The purpose of low-dose CT scans is to provide the most effective diagnostic imaging results without a decline in image quality, while eliminating artifacts and image noise. This is because in low-dose CT scans, the most important factor reducing diagnostic quality is image noise. The aim of our study was to achieve the maximum possible dose reduction. While iterative reconstruction algorithms (IRT) were previously expected to reduce radiation dose, eliminate artifacts, and provide images without increased noise, today, such diagnostic imaging performance is expected from artificial intelligence-based image reconstruction programs.

In our study, the deep learning-based noise reduction algorithm was observed to provide significant advantages over conventional iterative methods in terms of enhancing visual quality and achieving diagnostic adequacy at low doses. Similarly, in the review by Szczykutowicz et al., it was emphasized that deep learning-based CT reconstructions could reduce absolute noise in line with low-dose protocols while preserving image sharpness and avoiding “plastic” or “smudged” appearances (7).

In the qualitative visual evaluations, when assessed across the five parameters of lesion edge sharpness (LES), visibility of small structures (VSS), diagnostic reliability (DR), visual noise (VN), and artifacts (ART), significant differences were identified among the parameters. In most of these parameters, images obtained at the 45 mAs dose level were rated predominantly as “diagnostic” or “good quality,” indicating that this protocol could optimize image quality in patients with both low and high BMI values. In contrast, low-dose images obtained with the 30 mAs protocol exhibited serious limitations in diagnostic quality, and there were notable increases in edge blurring and reductions in the visibility of small structures. Nonetheless, in patients with BMI <30 kg/m², images obtained at 30 mAs were satisfactory in terms of some parameters, suggesting that low-dose 30 mAs imaging may be adequate in selected patient groups.

Although noise values increased significantly in both low-dose protocols, at the 45 mAs level, this increase did not adversely affect diagnostic visual evaluations. Overall, the results indicated that image quality depended not only on

technical parameters but also on the type of algorithm, dose level, and patient characteristics. This demonstrated that patient-specific dose optimization and algorithm selection play a critical role in diagnostic accuracy, particularly in lung diseases secondary to RA. In the objective mediastinal evaluations, significant differences were found between the standard scans and the low-dose 30 mAs and 45 mAs scans in the measurements performed in the parenchymal window (WL: -600, WW: 1600) and mediastinal window (WL: 300, WW: 1500) ($p < 0.001$). However, in visual scoring, no statistically significant difference was found between the standard scans and the low-dose 45 mAs scans in terms of LES, VSS, VN, ART, and DR, and the visual evaluation results of these two protocols were consistent.

In their study of abdominal CT images using the sinogram-affirmed iterative reconstruction algorithm (SAFIRE*), Choy et al. (2018) demonstrated that images obtained with 50% dose reduction had higher signal-to-noise ratio (SNR) and lower objective noise levels compared to images obtained with conventional weighted filtered back projection (wFBP) at 100% dose. It was emphasized that SAFIRE provided significant improvements in both quantitative and qualitative evaluations, particularly at higher strength levels (4 and 5) (8). In our study, when deep learning-based noise reduction was used in low-dose CT scans, diagnostic adequacy was maintained in some parameters even at 30 mAs, but in general, significant improvements in diagnostic reliability and visual quality were achieved at 45 mAs. Especially at the tracheal and aortic levels, noise values increased significantly in the

30 mAs protocol, and visual noise scores shifted to lower ratings. These results overlapped with those of Choy et al., showing that advanced iterative algorithms could reduce noise levels and preserve diagnostic quality in low-dose protocols. Although our study did not directly compare the deep learning-based algorithm used here to SAFIRE, the significant improvements in visual quality at 45 mAs highlighted the critical role of higher algorithmic processing power in producing high-quality images with dose reduction. In summary, both studies demonstrated that newly developed reconstruction methods could optimize diagnostic quality in CT imaging.

In the CNR evaluations in our study, it was determined that in the mediastinal window, the CNR values of the standard and Precise 45 mAs imaging protocols were similar, while Precise 30 mAs imaging showed significantly lower CNR values. In the parenchymal window, the Precise 30 mAs images showed significantly lower values than the Precise 45 mAs images, and the Precise 45 mAs images showed significantly lower values than the standard scans. In the phantom study conducted by Lee et al., increased noise and decreased SNR and CNR values were detected with the selected tube voltage and further radiation dose reduction. In their study, it was recommended to exercise caution regarding the risk of non-diagnostic image quality when the radiation dose was reduced by more than 60% compared to their reference values. In our study, the difference in CNR values between the standard imaging and Precise 45 mAs imaging protocols in the parenchymal window may be attributed to dose reduction beyond a

certain threshold, and it was considered that with slightly higher low-dose scans, standard imaging quality could also be achieved in the CNR parameter (9). In addition to this, devices such as dual-layer detector spectral CT scanners may allow standard-quality images to be obtained at lower doses (10).

In terms of BMI, in our study, no statistically significant difference was found between the <30 and ≥ 30 BMI groups in the visual evaluations of the 30 mAs and 45 mAs scan protocols. However, in a larger-population study, statistically significant differences may emerge. Lee et al. (2014) found that in ultra-low-dose imaging, image quality depended not only on patient body type but also on lesion type (9). In their ultra-low-dose CT study, Vardhanabbuti et al. (2017) showed that being overweight reduced pulmonary nodule detection rates due to increased image noise, and they concluded that such imaging was not suitable for overweight patients (11). In our study, no significant differences were found between the two dose levels in the examined parameters, which may also be related to lesion type, as reported by Lee et al. (2014) (9).

Ding et al. highlighted the diagnostic adequacy of ultra-low-dose spectral CT (ULDCT) in lung nodule screening, showing that electron density map (EDM) images obtained with advanced reconstruction techniques were satisfactory in terms of both subjective and objective quality (10). Similarly, in our study, when reconstruction algorithm quality was enhanced (Precise 45 mAs), visual evaluation scores increased significantly and achieved diagnostic value. The

achievement of high signal-to-noise and contrast-to-noise ratios with an average effective dose of 0.3 mSv in the study conducted by Ding et al., despite a 91.2% dose reduction, was compatible with our findings of dose reduction in low mAs protocols while maintaining significant visual scores. Furthermore, while EDM provided more pronounced contrast in subsolid nodules and ground-glass opacities in the study by Ding et al., in our study, low-dose protocols also provided sufficient information about LES and VSS. In both studies, modern reconstruction techniques were shown to compensate for the potential disadvantages of low doses, preserving diagnostic accuracy and even enhancing it in certain lesion subgroups.

In the review published by Power et al. in 2016, it was emphasized that the dramatic increase in CT usage over the years has been accompanied by a significant rise in the exposure of patients to ionizing radiation. The aforementioned study raised concerns that cumulative dose increases, even in low-dose CT examinations, may be associated with long-term cancer risk. At the same time, however, it was noted that advanced imaging systems, through reconstruction algorithms, could significantly reduce radiation doses without compromising image quality (12). In our study, similarly, the deep learning-based noise reduction algorithm was shown to provide adequate visual quality at lower doses compared to classical iterative methods. In our study, the mean total DLP value was 591.8 ± 199.7 mGy·cm in previous examinations, while in 30 mAs and 45 mAs scans, it was 62.4 ± 6.6 and 94.1 ± 11.0 mGy·cm, respectively. This parallelism demonstrates that technological

advancements provide tangible gains for patient safety not only in theory but also in practical clinical applications. Additionally, the principle emphasized by Power et al., namely the “balance between image quality and dose,” was also one of the arguments of our study, and in this context, both studies highlighted the importance of individualized imaging protocols (12).

Our study had certain limitations. First, the study was conducted with a retrospective design and in a single center. The relatively limited number of patients included in the study may have reduced the statistical power of the analyses performed, particularly in subgroups with BMI ≥ 30 , and this situation may have prevented the detection of significant differences in some comparisons. Furthermore, since the technical details of the deep learning-based noise reduction algorithm used in the study were presented by the manufacturer as proprietary information, limited information was available regarding the operational mechanism of the algorithm and the dataset on which it was trained. This situation makes it difficult to comment on the generalizability of the results obtained in this study. Finally, with additional analyses to be conducted at different dose ranges, researchers may evaluate whether the new algorithm yields results equivalent to the classical method also in terms of objective measurements.

Conclusion

In this study, which aimed to evaluate the balance between image quality and radiation dose in low-dose CT scans of patients diagnosed with RA, comprehensive analyses were performed using both visual

scoring and quantitative noise measurements. The results revealed that at the 45 mAs dose level, the deep learning-assisted reconstruction algorithm demonstrated performance comparable, and in some cases superior, to high-dose standard scan images in critical parameters such as lesion edge sharpness, visibility of small structures, and diagnostic reliability.


In the low-dose protocol at the 30 mAs level, on the other hand, marked decreases were observed in certain parameters related to diagnostic quality. Particularly weak results were obtained in lesion edge sharpness and visibility of small structures. Visual noise and artifact evaluations showed lower scores in this group, and accordingly, the level of diagnostic reliability also decreased. These results suggest that the 30 mAs protocol may not provide sufficient image quality for every patient, and more pronounced quality losses may occur in some patient groups as a secondary effect on multiple parameters.

In conclusion, the results of our study demonstrated that the deep learning-assisted low-dose CT protocol at the 45 mAs dose level is a preferable option in clinical practice in terms of both image quality and radiation safety. However, it was shown that scans at the 30 mAs level should be used with caution, and these protocols should be adapted according to patient characteristics. The data obtained here support the usability of low-dose CT in the follow-up of thoracic involvement associated with RA.

Conflicts of interest: There are no conflicts of interest to declare.

Funding: Not applicable (no funding was provided).

Ethical Statement: This retrospective study was approved by the Hatay Mustafa Kemal University ethics committee, and the requirement for informed consent was waived (30/04/2025, meeting no. 6, decision no. 39).

 Cite: Uçar, A., & Korkmaz, İ. (2026). Low-Dose CT in Lung Pathologies Related to Rheumatoid Arthritis: Comparison of Deep Learning-Based Noise Reduction Algorithm and Iterative Reconstruction Algorithm. *Acta Medica Young Doctors*, 2(3), 57–70.

References

1. Demirel A, Kirnap M. Romatoid Artrit Tedvisinde Geleneksel ve Güncel Yaklaşımlar. *Sağlık Bilimleri Dergisi* 2010;19:74-84.
2. Karazincir S, Akoğlu S, Güler H, Balci A, Babayiğit C, Eğılmez E. The evaluation of early pulmonary involvement with high resolution computerized tomography in asymptomatic and non-smoker patients with rheumatoid arthritis. *Tuberk Toraks* 2009;57:14-21.
3. Kelly BS, Judge C, Bollard SM, Clifford SM, Healy GM, Aziz A, et al. Radiology artificial intelligence: a systematic review and evaluation of methods (RAISE). *Eur Radiol* 2022;32:7998-8007. DOI: 10.1007/s00330-022-08784-6
4. Ozaki S, Haga A, Chao E, Maurer C, Nawa K, Ohta T, et al. Fast statistical iterative reconstruction for mega-voltage

computed tomography. *J Med Invest* 2020;67:30-9. DOI: 10.2152/jmi.67.30

5. Hackner K, Hütter L, Flick H, Grohs M, Kastrati K, Kiener H, et al. Screening for rheumatoid arthritis-associated interstitial lung disease-a Delphi-based consensus statement. *Z Rheumatol* 2024;83:160-8. DOI: 10.1007/s00393-023-01464-w

6. Brenner DJ, Hall EJ. Computed tomography--an increasing source of radiation exposure. *N Engl J Med* 2007;357:2277-84. DOI: 10.1056/NEJMra072149

7. Szczykutowicz TP, Toia GV, Dhanantwari A, Nett B. A review of deep learning CT reconstruction: concepts, limitations, and promise in clinical practice. *Curr Radiol Rep* 2022;10:101-15. DOI: 10.1007/s40134-022-00399-5

8. Choy S, Parhar D, Lian K, Schmiedeskamp H, Louis L, O'Connell T, et al. Comparison of image noise and image quality between full-dose abdominal computed tomography scans reconstructed with weighted filtered back projection and half-dose scans reconstructed with improved sinogram-affirmed iterative reconstruction (SAFIRE*). *Abdom Radiol* 2019;44:355-61. DOI: 10.1007/s00261-018-1687-9

9. Lee SW, Kim Y, Shim SS, Lee JK, Lee SJ, Ryu YJ, et al. Image quality assessment of ultra low-dose chest CT using sinogram-affirmed iterative reconstruction. *Eur Radiol* 2014;24:817-26. DOI: 10.1007/s00330-013-3090-9

10. Ding L, Chen M, Li X, Wu Y, Li J, Deng S, et al. Ultra-low dose dual-layer detector spectral CT for pulmonary nodule screening: image quality and diagnostic performance. *Insights Imaging* 2025;16:11. DOI: 10.1186/s13244-024-01888-1

11. Vardhanabhuti V, Pang CL, Tenant S, Taylor J, Hyde C, Roobottom C.

Prospective intra-individual comparison of standard dose versus reduced-dose thoracic CT using hybrid and pure iterative reconstruction in a follow-up cohort of pulmonary nodules-Effect of detectability of pulmonary nodules with lowering dose based on nodule size, type and body mass index. *Eur J Radiol* 2017;91:130-41. DOI: 10.1016/j.ejrad.2017.04.006

12. Power SP, Moloney F, Twomey M, James K, O'Connor OJ, Maher MM. Computed tomography and patient risk: Facts, perceptions and uncertainties. *World J Radiol* 2016;8:902-15. DOI: 10.4329/wjr.v8.i12.902